Pekola, J. P.; Torizuka, K.; Manninen, A. J.; Kyynäräinen, J. M.; Volovik, G. E.

Observation of a topological transition in the 3He-A vortices

Published in:
Physical Review Letters

DOI:
10.1103/PhysRevLett.65.3293

Published: 24/12/1990

Document Version
Publisher's PDF, also known as Version of record

Please cite the original version:
Pekola, J. P., Torizuka, K., Manninen, A. J., Kyynäräinen, J. M., & Volovik, G. E. (1990). Observation of a topological transition in the 3He-A vortices. *Physical Review Letters*, *65*(26), 3293-3296. https://doi.org/10.1103/PhysRevLett.65.3293

Observation of a Topological Transition in the ^{3}He-A Vortices

J. P. Pekola, K. Torizuka, A. J. Manninen, and J. M. Kyynäräinen
Low Temperature Laboratory, Helsinki University of Technology, 02150 Espoo, Finland

G. E. Volovik
L. D. Landau Institute for Theoretical Physics, U.S.S.R. Academy of Sciences, 117334 Moscow, U.S.S.R.
(Received 9 August 1990)

Vortices in ^{3}He-A in low magnetic fields ($H \leq 20$ mT) have been studied by ultrasonics. A first-order phase change between two vortex types, with dissimilar sound absorption, has been found. The magnetic field at the transition is on the order of the dipolar field H_d. The observed change occurs between continuous vortex textures with different topological charges in the $\hat{\mathbf{d}}$ field (where $\hat{\mathbf{d}}$ is the magnetic anisotropy vector).

PACS numbers: 67.50.−b

The unique property of superfluid ^{3}He-A is its ability to sustain continuous vorticity. In this respect ^{3}He-A differs from other known superfluids (^{4}He II, ^{3}He-B, and conduction electrons in superconductors) in which the superflow velocity $\mathbf{v}_s$ is potential and the vorticity $\nabla\times\mathbf{v}_s$ is concentrated in the hard cores of quantized vortices. Owing to a specific combination of spontaneously broken gauge and orbital symmetries, the vorticity of ^{3}He-A can be distributed continuously within the texture of the orbital vector $\hat{\boldsymbol{l}}$, according to the Mermin-Ho relation[1]

$$(\nabla\times\mathbf{v}_s)_z = (h/4\pi m_3)\hat{\boldsymbol{l}}\cdot(\partial_x\hat{\boldsymbol{l}}\times\partial_y\hat{\boldsymbol{l}})\,. \quad (1)$$

Depending on external conditions, a variety of periodic vortex textures can arise in ^{3}He-A under rotation. These differ from each other in their topology, symmetry, and number N of circulation quanta $h/2m_3$ per elementary cell of the vortex lattice.[2,3]

At a given temperature T and pressure p two more external parameters may affect the vortex textures: the angular velocity of rotation Ω, which determines the cross-sectional area per one quantum of circulation, $S = h/4m_3\Omega$, and the magnetic field $\mathbf{H}$, which interacts with the magnetic anisotropy vector $\hat{\mathbf{d}}$. For the latter case the relevant free-energy term is $F_{2H} = \frac{1}{2}(\chi_\perp - \chi_\parallel)(\hat{\mathbf{d}}\cdot\mathbf{H})^2$, where $\chi_\perp$ and $\chi_\parallel$ are the transverse and longitudinal susceptibilities, respectively. In its turn, the spin-orbit dipole-dipole interaction couples $\hat{\mathbf{d}}$ and $\hat{\boldsymbol{l}}$: $F_d = -g_d(\hat{\mathbf{d}}\cdot\hat{\boldsymbol{l}})^2$. As a result, the three length scales of importance are (1) dipolar length $\xi_d \simeq 10$ μm; (2) magnetic length $\xi_H = \xi_d H_d/H$, where H_d is the (dipolar) field, at which F_{2H} and F_d are of the same size ($H_d = 2$–5 mT); and (3) the "intervortex" distance $r_\Omega = S^{1/2}$, which is on the order of 100 μm at $\Omega = 1$ rad/sec.

Extensive NMR experiments on rotating ^{3}He-A have been performed in the range of 15–60 mT,[4] which is larger than H_d by a wide margin. In this region, where $\xi_H \ll \xi_d \ll r_\Omega$ and $\hat{\mathbf{d}}$ is practically forced into the plane perpendicular to $\mathbf{H}$, the so-called Seppälä-Volovik (SV) vortices were observed.[5] These are continuous structures, each with $N = 2$ quanta of circulation (4π vortices), for which all vorticity is concentrated in the soft core of radius $\sim\xi_d$, so that SV vortices are well separated from each other in the vortex lattice since $r_\Omega \gg \xi_d$ [see Fig. 1(a)]. Each SV vortex is characterized by the integer topological invariant of the $\hat{\boldsymbol{l}}$ field, viz.,

$$\tilde{m}_l = (1/4\pi)\int_\sigma \hat{\boldsymbol{l}}\cdot(\partial_x\hat{\boldsymbol{l}}\times\partial_y\hat{\boldsymbol{l}})\,dx\,dy\,. \quad (2)$$

This winding number shows how many times $\hat{\boldsymbol{l}}$ covers the unit sphere when the elementary cell σ of the vortex lattice is swept. According to the Mermin-Ho relation, Eq. (1), $\tilde{m}_l = N/2$ for a continuous vortex texture. Therefore, $\tilde{m}_l = 1$ for the SV 4π vortex, i.e., inside the soft core of the SV vortex the $\hat{\boldsymbol{l}}$ texture sweeps the unit sphere once.

One may construct a similar invariant for the $\hat{\mathbf{d}}$ vector field in the unit cell,[2]

$$\tilde{m}_d = (1/4\pi)\int_\sigma \hat{\mathbf{d}}\cdot(\partial_x\hat{\mathbf{d}}\times\partial_y\hat{\mathbf{d}})\,dx\,dy\,, \quad (3)$$

but, contrary to $\tilde{m}_l$, $\tilde{m}_d$ is not related to N. In particu-

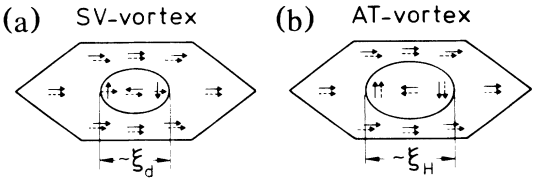

FIG. 1. (a) Schematic illustration of the SV high-field dipole-unlocked vortex ($\xi_H < \xi_d$) and (b) of the AT low-field dipole-locked vortex ($\xi_H > \xi_d$). In both structures the vorticity is concentrated in the soft cores of size ξ_d and ξ_H, respectively. The $\hat{\boldsymbol{l}}$ vector (solid arrows) sweeps the unit sphere inside the soft core. The $\hat{\mathbf{d}}$ vector (dashed arrows) sweeps the unit sphere only in the dipole-locked AT vortex, $\tilde{m}_d = 1$, while in the SV vortex $\tilde{m}_d = 0$ and the $\hat{\mathbf{d}}$ field is uniform. The phase transition between the SV and AT vortices at $\xi_H \sim \xi_d$ is of topological nature, with a discontinuous jump in the topological charge $\tilde{m}_d$.

lar, $\tilde{m}_d \equiv 0$ for the SV vortex since $\hat{\mathbf{d}}$ is forced into the transverse plane.

The situation should be different when $H \ll H_d$, where $\xi_H \gg \xi_d$ and the $\hat{\mathbf{d}}$ field prefers to follow $\hat{\boldsymbol{l}}$, i.e., it is dipole locked [see Fig. 1(b)]. We discuss only the two main dipole-locked textures that satisfy the Mermin-Ho relation, both with $\tilde{m}_l/N = \frac{1}{2}$. One is the lattice of Anderson-Toulouse (AT) 4π vortices[6] with $\tilde{m}_l = 1$ and $N = 2$ per unit cell, the other is a lattice whose unit cell consists of four 2π Mermin-Ho (MH) vortices[7] with $\tilde{m}_l = 2$ and $N = 4$. It is important to note that in both cases $\hat{\mathbf{d}}$ must follow $\hat{\boldsymbol{l}}$ and, therefore, for these dipole-locked vortex textures $\tilde{m}_d = \tilde{m}_l$.

This means that at an intermediate field, $H = H_c \simeq H_d$, one should expect a phase transition between dipole-unlocked high-field vortices and dipole-locked low-field vortices.[2] Since these textures have different topological charges $\tilde{m}_d$ per circulation quantum, the transition can be only of first order; $\tilde{m}_d/N$ changes discontinuously from $\frac{1}{2}$ at $H < H_c$ to 0 at $H > H_c$. The critical field H_c should be virtually unaffected by Ω as long as $\xi_d < r_\Omega$ ($\Omega < 10^1$-10^2 rad/sec); experimentally the inequality is always fulfilled. We now discuss this topological transition as first observed in our ultrasonic experiment.

The measurements were carried out in Helsinki using our second rotating cryostat ROTA2.[8] We employed pulsed sound transmission techniques. Our experimental cell has two X-cut quartz crystals, $L = 4$ mm apart. The diameter of the cylindrical ^{3}He volume is 6 mm and the fluid in the cell is in liquid contact with the main ^{3}He reservoir through several 1×1-mm^2 holes at both ends of a quartz spacer. Sound pulses at $f = 26.8$ and 44.7 MHz frequencies were employed. A superconducting solenoid outside the sound cell provided an axial magnetic field $\mathbf{H}$. In a few runs, a transverse magnetic field was used, produced by a large saddle coil in the surrounding helium bath.

Expecting metastability effects in the predicted first-order textural transition, we started our experiments by applying the following sequence [see Fig. 2(a)]: Initially, the sample of ^{3}He-A was cooled to $T/T_c \simeq 0.9$ in a magnetic field of 2.2 mT. After stabilizing the temperature, the cryostat was set into rotation at $\Omega = 0.3$ rad/sec. Thereafter, H was linearly reduced from 2.2 mT to 0 in 8 min. In Fig. 2(b), the upper curve (labeled 1) shows the reduced sound amplitude $A/A(T_c)$ at $f = 26.8$ MHz during this sweep; A is related to the attenuation α via the dependence $A \propto \exp(-\alpha L)$. Next, at $t = 11$ min, the cryostat was stopped and, after 1 min, reaccelerated to $\Omega = 0.3$ rad/sec. H was then swept from 0 to 2.2 mT, again in 8 min [see Fig. 2(a)]. During this sweep [curve 2 in Fig. 2(b)], A showed considerable hysteresis with respect to the signal obtained from the state that had been created in the 2.2-mT field.

This initial experiment already yielded important data on the existing vortex states in ^{3}He-A: First, there seemed to be at least two types of vortices, separated by

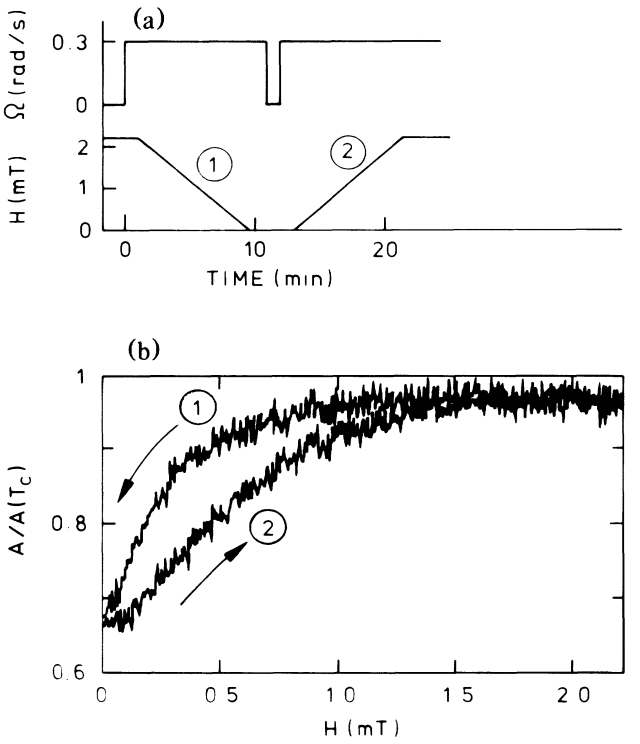

FIG. 2. (a) Sequence of Ω and H, explained in the text. (b) Hysteretic change in the amplitude A of zero sound, in relation to its value $A(T_c)$ at the critical temperature, during a slow magnetic-field sweep under rotation.

a transition at $H \leq 2$ mT. Second, the hysteresis implied that we are dealing with a first-order phase change, as expected.

Figure 3 shows data at $f = 26.8$ MHz from a measurement to investigate the stability of the low-H vortex at $p = 26.7$ bars and $T/T_c = 0.9$. The inset in Fig. 3(c) illustrates the measuring sequence on the (H, Ω) plane. Initially, the sample was accelerated at $H = 0$ to a rotation velocity Ω_0 (0–3.5 rad/sec). Following this, a small axial magnetic field, $H_{\rm ref} \simeq 0.5$ mT, was applied and the sound amplitude $A_{\rm ref}$ was measured. Next, H was swept up to $H_{\rm max}$ and then back to $H_{\rm ref}$ while the cryostat was continuously rotated at $\Omega = \Omega_0$. A new measurement of A at $H_{\rm ref}$ then yielded information on the persistence of the low-field vortices: If the signal remained the same, the low-field vortices were still present in the experimental chamber, but if A had changed, they had lost their stability against high-field vortices during the field sweep. Figure 3 shows that a different signal appeared, at all experimentally used speeds of rotation, when $H_{\rm max}$ exceeded $H_{c1} = 4$ mT, i.e., H_{c1} is the catastrophe field at which the low-field vortices become unstable.

The opposite check, a test for the stability of high-field vortices, was done as follows: The reference sound amplitude was first measured when high-field vortices were created at $H \simeq 2.5$ mT. This value was then compared with A obtained after successive sweeps of H from 2.5

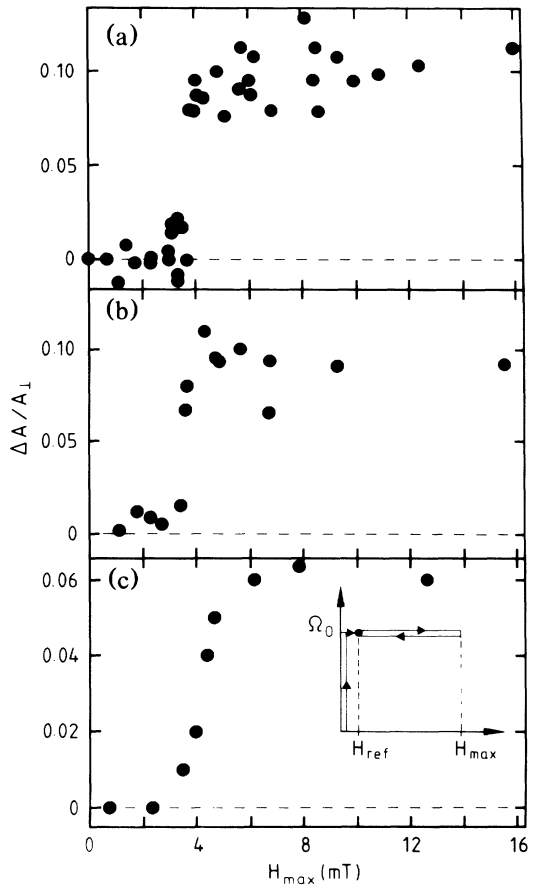

FIG. 3. Measurements on the stability of the low-field vortex: (a) $\Omega = 1.0$ rad/sec, (b) 2.0 rad/sec, and (c) 3.5 rad/sec. In each case $f = 26.8$ MHz. The inset in (c) illustrates the experimental sequence; in all cases $\mathbf{H}$ was parallel to $\boldsymbol{\Omega}$. The data points show the change in sound amplitude, $\Delta A = A_{\rm ref}(\text{after}) - A_{\rm ref}(\text{before})$, during experimental sequences in which A was measured at $H = H_{\rm ref}$ before and after sweeping the magnetic field to $H_{\rm max}$. The data are reduced by $A_\perp$, the sound amplitude in stationary liquid when $\hat{\boldsymbol{l}} \perp \hat{\mathbf{z}}$.

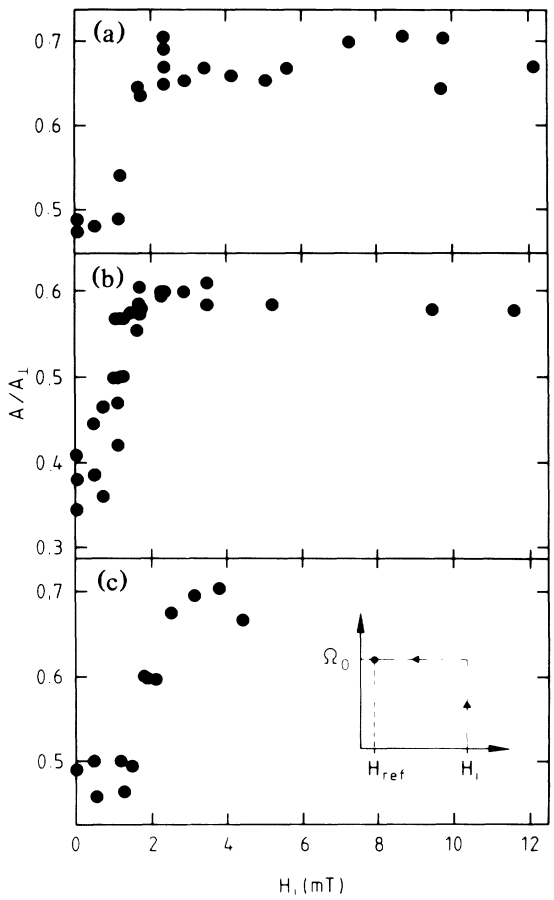

FIG. 4. Measurements to determine H_c at the thermodynamic transition. The data points show the reduced amplitude $A/A_\perp$ measured at $H = H_{\rm ref}$, as a function of the magnetic field H_i at which the rotation was started. (a) $\mathbf{H}_i \| \boldsymbol{\Omega} \| \hat{\mathbf{q}}$, $\Omega = 0.3$ rad/sec, (b) $\mathbf{H}_i \| \boldsymbol{\Omega} \| \hat{\mathbf{q}}$, $\Omega = 1.0$ rad/sec, and (c) $\mathbf{H}_i \perp \boldsymbol{\Omega} \| \hat{\mathbf{q}}$, $\Omega = 0.3$ rad/sec. In each case $f = 26.8$ MHz. The measuring sequence is seen in the inset of (c) and explained in the text.

mT to zero and back to 2.5 mT, during continuous rotation. No change in A was observed, which demonstrated the stability of the high-field vortices down to $H = 0$. In this experiment, $f = 44.7$ MHz was used because at this frequency the attenuation levels of the low- and high-field vortices at $H = 2.5$ mT were more clearly different than at $f = 26.8$ MHz.

The true thermodynamic transition curve $H_c(\Omega)$ was found by the experimental sequence shown in the inset of Fig. 4(c). Initially, the cryostat was set into rotation at $H = H_i$. The field was then swept to $H = H_{\rm ref} \simeq 0.5$ mT. A series of measurements of A at $H_{\rm ref}$, with different values of H_i, then allowed us to determine the true H_c. If $H_i < H_c$, only the low-field vortices existed during this procedure. If $H_i > H_c$, high-field vortices were created initially and, since they are metastable at low fields, they persisted during our experimental procedure. Figure 4 shows that the sound amplitude at $H_{\rm ref}$ is different for H_i below and above $H_c \simeq 1.5$ mT. The transition is not as sharp as in the measurement of Fig. 3, because the low-field state ($H_i \leq 1.5$ mT) can be a mixture of low- and high-field vortices.

The amplitudes of low- and high-field phases in Fig. 4 equal those of Fig. 3 (A is not directly shown in Fig. 3), thus showing that we are dealing, in both cases, with the same states. The magnetic field separating them, $H_c \simeq 1.5$ mT, was the same for all experimental values of Ω (0.15–3.5 rad/sec). This independence on Ω is what was expected for the critical field H_c of the topological transition. A measurement where $\mathbf{H}_i$ was perpendicular to the propagation direction $\hat{\mathbf{q}}$ of the ultrasound is shown in Fig. 4(c); the result is similar to that of parallel orientation in Fig. 4(a).

We are now ready to sketch, in Fig. 5, the phase diagram of the vortex textures in ^{3}He-A in low and intermediate magnetic fields. When $H \leq H_c$, the low-field

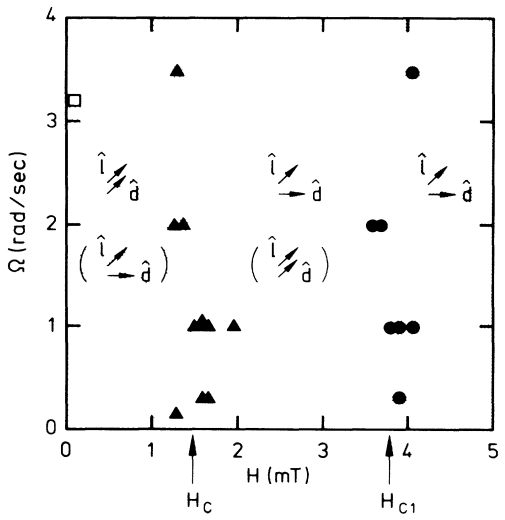

FIG. 5. Experimental phase diagram of vortex textures in ^{3}He-A in low magnetic fields. The symbol with $\hat{l}$ and $\hat{\mathbf{d}}$ not aligned depicts the dipole-unlocked state [Fig. 1(a)], while the one with $\hat{l}$ and $\hat{\mathbf{d}}$ aligned refers to the dipole-locked state [Fig. 1(b)]. The symbols without parentheses are stable structures, the ones in parentheses are metastable. $H_c(\Omega)$ (triangles) shows the measured critical field of the thermodynamic first-order transition between the vortex states, while H_{c1} (solid circles) defines the catastrophe line at which the low-field vortices lose their stability.

vortex is stable. At $H_c < H < H_{c1}$, both kinds of vortices can exist, but the low-field vortex is metastable. When $H > H_{c1}$, only the high-field vortex is present. The open square in Fig. 5, at $H \simeq 0$, marks a critical rotation speed at which we have observed a sudden increase in sound absorption upon accelerating the cryostat. This may be attributed to a transition between different types of dipole-locked vortices.

The magnetic-field dependence of the AT vortex core size provides us with qualitative understanding of the observed attenuation levels. In the stationary state a magnetic field $\mathbf{H} \| \hat{\mathbf{z}}$ orients $\hat{l} \perp \hat{\mathbf{z}}$. In this case we denote $A = A_\perp$. Owing to the anisotropy of sound propagation, any deviation from this "planar" texture yields, under these conditions, higher attenuation, i.e., lower A. The difference $A_\perp - A$ is proportional to the area where vector $\hat{l}$ deviates from the transverse plane and, therefore, to the relative cross-sectional area of the soft cores. For the dipole-locked AT vortices, $A_\perp - A$ is proportional to $(\xi_H/r_\Omega)^2 = (\xi_d/r_\Omega)^2 (H_d/H)^2$ at $\xi_d < \xi_H \ll r_\Omega$ and saturates at $\xi_H \sim r_\Omega$. This behavior is different for dipole-unlocked SV vortices, which have the core size of order ξ_d, thus yielding a smaller value of $A_\perp - A$, in agreement with Figs. 2 and 4. A detailed numerical analysis of the AT and SV vortex structures in the whole experimental range of magnetic fields is needed before one can make quantitative comparisons of the attenuation levels.[9]

We thank O. V. Lounasmaa and M. M. Salomaa for useful discussions. This work was supported by the Academy of Finland and by the U.S.S.R. Academy of Sciences through project ROTA, and by the Körber-Stiftung of Hamburg, Germany. One of us (A.J.M.) acknowledges a scholarship from the Emil Aaltonen Foundation.

[1]N. D. Mermin and T.-L. Ho, Phys. Rev. Lett. **36**, 594 (1976).

[2]M. M. Salomaa and G. E. Volovik, Rev. Mod. Phys. **59**, 533 (1987).

[3]A. L. Fetter, in *Progress in Low Temperature Physics*, edited by D. F. Brewer (North-Holland, Amsterdam, 1986), Vol. 10, p. 1.

[4]H. K. Seppälä, P. J. Hakonen, M. Krusius, T. Ohmi, M. M. Salomaa, J. T. Simola, and G. E. Volovik, Phys. Rev. Lett. **52**, 1802 (1984).

[5]H. K. Seppälä and G. E. Volovik, J. Low Temp. Phys. **51**, 279 (1983).

[6]G. E. Volovik and N. B. Kopnin, Pis'ma Zh. Eksp. Teor. Fiz. **25**, 26 (1977) [JETP Lett. **25**, 22 (1977)].

[7]T. Fujita, M. Nakahara, T. Ohmi, and T. Tsuneto, Prog. Theor. Phys. (Japan) **60**, 671 (1978).

[8]R. H. Salmelin, J. M. Kyynäräinen, M. P. Berglund, and J. P. Pekola, J. Low Temp. Phys. **76**, 83 (1989).

[9]M. M. Salomaa (to be published).